# Selective regulation of long-form calcium-permeable AMPA receptors by an atypical TARP $\gamma$-5

David Soto, Ian D. Coombs, Massimiliano Renzi, Marzieh Zonouzi,
Mark Farrant and Stuart G. Cull-Candy

Department of Neuroscience, Physiology and Pharmacology
University College London, Gower Street, London WC1E 6BT U.K.

## 1 Supplementary Methods

### 1.1 Heterologous expression

Recombinant receptors were expressed in tsA201 cells (a gift from Raquel Yustos, Imperial College London) grown as previously described [1]. Transient transfection of receptor subunit and TARP combinations (plus EGFP) was performed using Lipofectamine 2000 (Invitrogen), according to the manufacturer's instructions. For homomeric receptors, cells were transfected at a ratio of 1:1 (AMPAR subunit:TARP); for heteromeric receptors, the transfection ratio was 1:1:2 (subunit:subunit:TARP; except where indicated). In each case, total DNA was 0.8 $\mu$g. Cells were split and plated on glass coverslips after 18–24 hours and recordings were made after a further 24–72 hours. In some cases, cells were maintained in 20 $\mu$M 6-cyano-7-nitroquinoxaline-2,3-dione (CNQX; Tocris Bioscience, Bristol, UK) to avoid AMPAR-mediated toxicity.

### 1.2 Receptor and TARP mutagenesis

Mutagenesis was performed using PCR, with mismatch primers obtained from Sigma Genosys (Poole, UK):

GluR1$_{S831A}$: GATCCCACAGCAAGCCATCAATGAAGCC and
GGCTTCATTGATGGCTTGCTGTGGGATC
$\gamma$-5$_{(1\text{-}206)}$: GAGGTATACTGCTTAGGACATGTACAGGC and
GCCTGTACATGTCCTAAGCAGTATACCTC.

The YFP-$\gamma$-5 fusion protein (YFP preceding $\gamma$-5 N-terminus) was created by inserting full-length $\gamma$-5 in-frame into the eYFP-tub vector (gift from Alastair Hosie, UCL), with a 7 amino-acid linker: SGLRLRG. All PCR was performed using Phusion polymerase (Finnzymes; Espoo, Finland).

### 1.3 Electrophysiology

Cells were viewed with a fixed stage upright microscope (Axioskop FS1; Zeiss, Welwyn Garden City, UK or Olympus BX51 WI; Olympus, London, UK) and EGFP-positive cells were selected for patch-clamp recording. Macroscopic currents were recorded at room temperature (22–25

°C) from outside-out membrane patches or from isolated whole cells using an Axopatch 200A amplifier and acquired using a Digidata 1200 interface board and pClamp software (Molecular Devices Corporation, Sunnyvale, CA).

### 1.4 Fast agonist application to excised patches

Outside-out patches were obtained using electrodes fabricated from borosilicate glass (1.5 mm o.d., 0.86 mm i.d.; Harvard Apparatus, Edenbridge, UK) with a resistance of 8–12 MΩ. Rapid solution switching at the patch was achieved by piezoelectric translation of an application tool as described previously [1]. The tool was made from theta glass (2 mm o.d.; Hilgenberg GmbH, Malsfeld, Germany) pulled to a tip opening of 200 $\mu$m, and was mounted on a piezoelectric translator (Burleigh LSS-3000/PZ-150M; EXFO Life Sciences & Industrial Division, Mississauga, Ontario or P-265.00, Physik Instrumente, Waldbronn, Germany). Control and agonist solutions flowed continuously through the two barrels and solution exchange occurred when movement of the translator was triggered by a voltage step (pClamp). To enable visualization of the solution interface and allow measurement of solution exchange 2.5 mg/ml sucrose was added to the agonist solution and the control solution was diluted by 5%. Recorded currents were low-pass filtered at 10 kHz and digitized at 20 or 50 kHz. At the end of each experiment, the adequacy of the solution exchange was assessed by destroying the patch and measuring liquid-junction current at the open pipette; the 10–90% risetime was always <200 $\mu$s [1].

### 1.5 Non-stationary fluctuation analysis (NSFA)

To deduce channel properties from macroscopic responses, glutamate (10 mM) was applied to outside-out patches (100 ms duration, 1 Hz) and the ensemble variance of all successive pairs of current responses calculated using IGOR Pro 5.05 (Wavemetrics, Lake Oswego, OR) and NeuroMatic (http://www.neuromatic.thinkrandom.com). The single-channel current ($i$), total number of channels ($N$) and maximum open probability ($P_{o,\,\mathrm{peak}}$) were then determined by plotting this ensemble variance ($\sigma^2$) against mean current ($\bar{I}$) and fitting with a parabolic function:

$$\sigma^2 = iI - \bar{I}^2/N + \sigma_B^2 \tag{1}$$

where $\sigma_B^2$ is the background variance. Along with expected peak-to-peak variation in the currents due to stochastic channel gating, some patches showed gradual changes in peak amplitude. In all cases, the mean response was calculated from epochs containing 20–200 stable responses, which were identified by using a Spearman rank-order correlation test (NeuroMatic). The weighted-mean single-channel conductance was calculated from the single-channel current and the holding potential (corrected for the calculated liquid-junction potential). $P_{o,\,\mathrm{peak}}$ was estimated by dividing the average peak current by $iN$.

### 1.6 Comparison of AMPAR deactivation and BGC quantal event decay

AMPAR deactivation, measured at room temperature (22–25 °C) in response to 1 ms applications of 1 mM glutamate in the presence of 50 $\mu$M cyclothiazide was fit with a double exponential

and the weighted time constant calculated [1]. The decay time constants of quantal events recorded from BGCs by Matsui et al. [2] (in the presence of 5 mM $Sr^{2+}$ and 200 $\mu$M CTZ at a median temperature of 33.5 °C) were 1.1 ms (climbing fiber stimulation) and 1.4 ms (parallel fiber stimulation). As our recordings of recombinant receptors were made at room temperature (median 23.5 °C), temperature-dependent scaling of the decay times was determined according to the equation:

$$Q_{10} = \left( \frac{R_{\mathrm{T}_1}}{R_{\mathrm{T}_2}} \right)^{\left( \frac{10}{\mathrm{T}_2 - \mathrm{T}_1} \right)} \tag{2}$$

where $Q_{10}$ is the temperature coefficient, $R_{\mathrm{T}_1}$ is the rate at temperature $\mathrm{T}_1$ and $R_{\mathrm{T}_2}$ is the rate at temperature $\mathrm{T}_2$ (R=1/decay time constant). Using $Q_{10}$ values of 1.5 [3] and 1.7 [4], the expected range of decay times at 23.5 °C was calculated to be 1.7 to 2.4 ms (**Fig.6c**).

### 1.7 Acute cerebellar slices

Mice, aged between postnatal days 34 and 49 (P34-49), were anaesthetized with isoflurane and decapitated. The brains were removed and dissected in cold (0.5–4 °C) oxygenated slicing solution, containing (in mM): 85 NaCl, 2.5 KCl, 0.5 $CaCl_2$, 4 $MgCl_2$, 25 $NaHCO_3$, 1.25 $NaH_2PO_4$, 75 sucrose, 25 glucose, 0.01 D-(-)2-amino-5-phosphonopentanoic acid (D-AP5); pH 7.4, when bubbled with 95% $O_2$ and 5% $CO_2$. Parasagittal slices (250 $\mu$m) were cut from the cerebellar vermis using a moving blade microtome (HM 650V; Microm International GmbH, Walldorf, Germany). Slices were incubated at 32 °C for 40 minutes and thereafter at room temperature, during which time the sucrose containing slicing solution was gradually replaced by a standard external solution containing (in mM): 125 NaCl, 2.5 KCl, 2 $CaCl2_2$, 1 $MgCl_2$, 25 $NaHCO_3$, 1.25 $NaH_2PO_4$, and 25 glucose; pH 7.4, when bubbled with 95% $O_2$ and 5% $CO_2$.

## References

[1] Soto, D., Coombs, I. D., Kelly, L., Farrant, M. & Cull-Candy, S. G. Stargazin attenuates intracellular polyamine block of calcium-permeable AMPA receptors. *Nat. Neurosci.* **10**, 1260-1267 (2007).

[2] Matsui, K., Jahr, C. E. & Rubio, M. E. High-concentration rapid transients of glutamate mediate neural-glial communication via ectopic release. *J. Neurosci.* **25**, 7538-7547 (2005).

[3] Veruki, M. L., Morkve, S. H. & Hartveit, E. Functional properties of spontaneous EPSCs and non-NMDA receptors in rod amacrine (AII) cells in the rat retina. *J. Physiol.* **549**, 759-774 (2003).

[4] Silver, R. A., Colquhoun, D., Cull-Candy, S. G. & Edmonds, B. Deactivation and desensitization of non-NMDA receptors in patches and the time course of EPSCs in rat cerebellar granule cells. *J. Physiol.* **493**, 167-173 (1996).

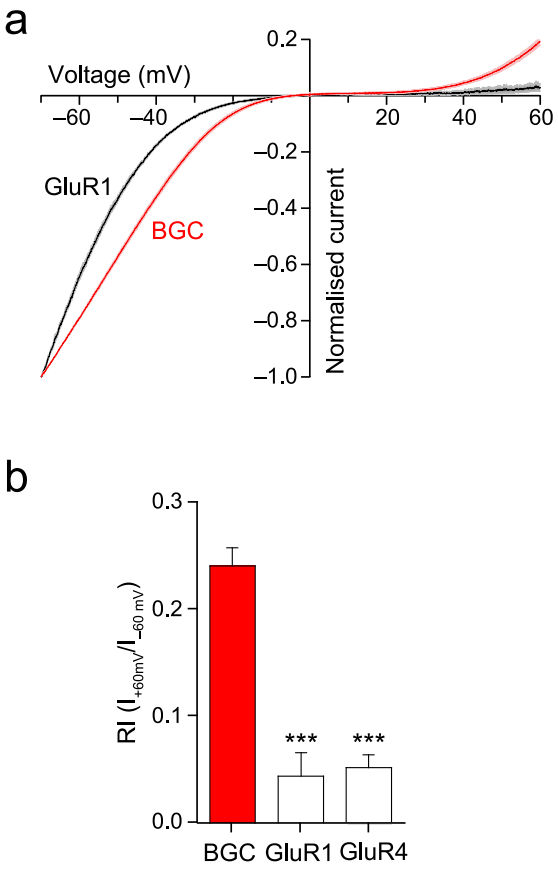


**Figure S1 Rectification of AMPAR-mediated whole-cell currents from BGCs in culture suggests a functional role for a TARP**. (**a**) A comparison of mean ramp *I-V*s recorded from BGCs (1-6 DIV, $n$ = 14) and tsA201 cells expressing homomeric GluR1 AMPARs ($n$ = 6) in response to bath application of 1 mM glutamate plus 50 $\mu$M cyclothiazide. Solid lines denote averages and shaded areas (evident only at positive voltages) indicate $\pm$ s.e.m. (**b**) The rectification index (RI; calculated as current at +60 mV/–60 mV) for AMPAR-mediated currents recorded from BGCs differed significantly from that of recombinant homomeric GluR1 and GluR4 responses ($n$ = 6 and 7, respectively). Asterisks denote significance (*** $P$<0.0005).

a

| | Surface expression (% of input) | |
|---|---|---|
| | Control ($n$) | Plus γ-5 ($n$, $P$) |
| GluR1 | 36 ± 4 (3) | 23 ± 3 (3, 0.0785) |
| GluR2(R) | 58 ± 6 (3) | 70 ± 6 (3, 0.2235) |
| GluR2(Q) | 66 ± 17 (3) | 6 ± 3 (3, 0.0259) * |
| GluR2L(Q) | 86 ± 7 (4) | 54 ± 10 (4, 0.0441) * |
| GluR4 | 74 ± 14 (3) | 56 ± 16 (3, 0.4302) |

b

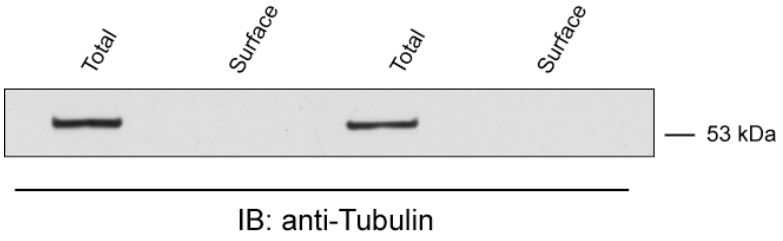


**Figure S2 Biotinylation reveals a $\gamma$-5-induced decrease in surface expression of GluR2(Q) and -2L(Q) but no significant change for GluR1, -2R or 4**. (**a**) Table showing the effects of $\gamma$-5 co-expression on the surface expression of various homomeric AMPARs. Values are densitometric measurements of surface protein expressed as a percentage of the input lane (input 2% of total, as shown in Fig. 8). Numbers show mean $\pm$ s.e.m. and the $P$ values (un-paired Student's $t$-test) for 3 or 4 repeated experiments (as indicated). The asterisks denote significance ($P<0.05$). (**b**) Western blot (from same gel illustrated in Fig. 8 for GluR2(R)) showing that, under conditions that label surface AMPARs, biotin does not bind the intracellular protein tubulin.

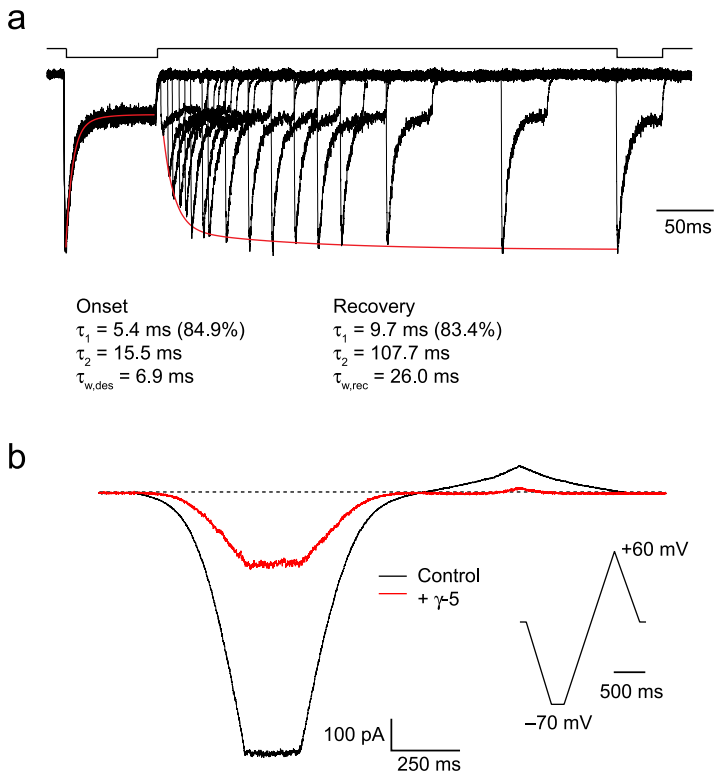


**Figure S3 Decreased steady-state whole-cell currents with $\gamma$-5 reflect a decrease in surface receptors**. (**a**) Representative traces showing the recovery from desensitization of GluR2(Q) AMPARs. Channels were activated with a 100 ms conditioning application of 1 mM glutamate, followed after a variable delay (2–400 ms) by a test pulse (1 mM, 50 ms). For clarity, not all responses are shown. The onset of desensitization was determined from a double exponential fit (red line) to the averaged conditioning response. Recovery from desensitization was determined from a fit to the peak of the test responses. Weighted time constants for desensitization ($\tau_{\mathrm{w,des}}$) and recovery ($\tau_{\mathrm{w,rec}}$) were determined from the fits, and the fractional steady state currents by dividing the asymptote of the fit by the peak of the conditioning response. For GluR2(Q) alone, ($\tau_{\mathrm{w,des}}$) was 7.44 $\pm$ 0.75 ms ($n$ = 4). In the presence of $\gamma$-5 this was unaltered (7.56 $\pm$ 0.18 ms, $n$ = 5, $P$ = 0.97). Similarly, $\gamma$-5 failed to alter the kinetics of recovery ($\tau_{\mathrm{w,rec}}$ was 15.0 $\pm$ 1.6 ms for GluR2(Q) and 19.0 $\pm$ 2.4 ms for GluR2(Q) plus $\gamma$-5, $P$ = 0.24). The steady state current was decreased in the presence of $\gamma$-5 (17.0 $\pm$ 3.4 % *versus* 29.9 $\pm$ 5.8 %, $n$ = 4 and 5 respectively, $P$ = 0.039). (**b**) Representative whole-cell voltage ramp responses (–70 mV to +60 mV, inset) recorded on bath application of 1 mM glutamate to tsA201 cells expressing GluR2(Q), either alone or with $\gamma$-5. 100 $\mu$M spermine was added to the pipette solution. In the presence of $\gamma$-5 the steady-state current (at –70 mV) was decreased to 20% of control (see Fig. 8d). This decrease was much larger than the decrease in fractional steady state current seen in isolated patches (57% of control, see above). When considered together with the fact that $\gamma$-5 failed to change the $P_{o,\mathrm{peak}}$ (Fig. 7c) and increased the single-channel conductance (Fig. 7b), the substantial decrease in whole-cell current density produced by $\gamma$-5 must result from a decrease in surface receptors.

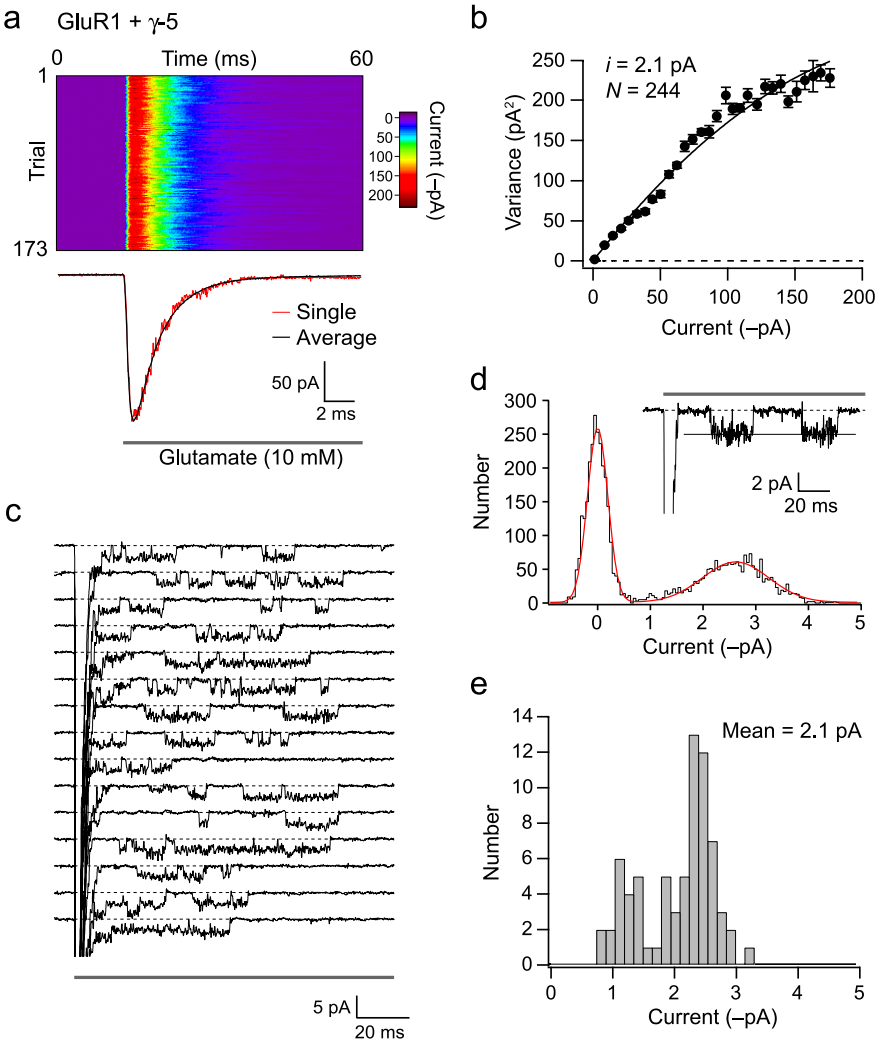


**Figure S4 Similarity of conductance estimates from NSFA and resolvable channel events suggest a homogeneous population of 'TARPed' receptors**. (**a**) Colour-coded image showing an array of responses (–60 mV, filtered at 10 kHz, sampled at 50 kHz) to rapid application of 100 mM glutamate (solid line) evoked from patches taken from tsA201 cells transfected with GluR1 and γ-5. The lower panel shows the average response (black) and an individual response (red). (**b**) Current-variance relationship generated from the recordings shown in a. For this patch, the fitted parabola (see Supplementary Methods, above) gave estimates of weighted mean single-channel current ($i$) and number of channels ($N$) of 2.1 pA and 244. The dashed line denotes background variance. (**c**) Selected traces taken from a, in which channel events were clearly resolved in the current record (for display and subsequent analysis the traces were digitally filtered at 2 kHz). Note the prolonged channel openings following decay of the macroscopic current (peak truncated). The solid line denotes the period of glutamate application. (**d**) All-point histogram of events in the tail of a single record (inset). The histogram is fitted with two Gaussians (red), representing the baseline and open channel current (dotted and thin solid line in inset). (**e**) Histogram of pooled single-channel current values (estimated as in d) giving a mean of 2.1 pA (38 pS).

| | Conductance (pS) ($n$, $P$) | $P_{o,\max}$ ($n$, $P$) | $\tau_{des}$ (ms) ($n$, $P$) | RI (+60mV/–80mV) ($n$, $P$) |
|---|---|---|---|---|
| GluR4 | 20.1 ± 1.3 (8) | 0.57 ± 0.03 (8) | 3.5 ± 0.27 (8) | 0.025 ± 0.003 (5) |
| + γ-2 | 31.4 ± 2.5 (9, 0.0016) | 0.61 ± 0.03 (9, 0.4644) | 5.7 ± 0.7 (9, 0.0114) | 0.238 ± 0.032 (4, 0.0001) |
| + γ-3 | 33.0 ± 1.3 (9, <0.0001) | 0.58 ± 0.06 (9, 0.9415) | 5.4 ± 0.3 (9, 0.0001) | 0.320 ± 0.032 (4, <0.0001) |
| + γ-4 | 34.2 ± 3.3 (10, 0.0024) | 0.55 ± 0.06 (10, 0.7617) | 11.7 ± 2.5 (10, 0.0090) | 0.176 ± 0.018 (5, <0.0001) |
| + γ-5 | 36.0 ± 2.6 (7, <0.0001) | 0.33 ± 0.03 (7, <0.0001) | 3.0 ± 0.2 (7, 0.1731) | 0.081 ± 0.012 (5, 0.0019) |
| + γ-7 | 33.1 ± 2.8 (5, 0.0005) | 0.65 ± 0.05 (5, 0.1794) | 3.3 ± 0.4 (5, 0.6525) | 0.141 ± 0.017 (8, 0.0003) |
| + γ-8 | 37.3 ± 3.1 (8, 0.0002) | 0.64 ± 0.05 (8, 0.2870) | 7.8 ± 1.8 (8, 0.0354) | 0.208 ± 0.022 (5, <0.0001) |

**Table S1** The effects of various TARPs on the properties of homomeric GluR4 AMPARs expressed in tsA201 cells (see Figs. 1–3).

| | | Conductance (pS) | RI (+60mV/–60mV) | *n* |
|---|---|---|---|---|
| GluR4 | | 20.1 ± 1.3 | 0.060 ± 0.006 | 8,5 |
| GluR4 + γ-5 | | 36.0 ± 2.6 | 0.153 ± 0.025 | 7,5 |
| GluR2/4 | Low RI | 13.4 ± 2.3 | 0.266 ± 0.041 | 8 |
| | Med RI | 8.0 ± 0.8 | 0.610 ± 0.043 | 6 |
| | High RI | 6.0 ± 1.1 | 1.021 ± 0.097 | 6 |
| GluR2/4 + γ-5 | Low RI | 27.1 ± 2.6 | 0.267 ± 0.025 | 7 |
| | Med RI | 15.4 ± 1.5 | 0.558 ± 0.040 | 9 |
| | High RI | 8.7 ± 1.1 | 0.895 ± 0.042 | 10 |
| GluR2L/4 | Low RI | 16.3 ± 2.5 | 0.237 ± 0.037 | 8 |
| | Med RI | 8.4 ± 1.3 | 0.676 ± 0.035 | 9 |
| | High RI | 6.7 ± 1.0 | 0.920 ± 0.044 | 6 |
| GluR2L/4 + γ-5 | Low RI | 30.9 ± 2.5 | 0.263 ± 0.028 | 7 |
| | Med RI | 21.2 ± 1.5 | 0.503 ± 0.027 | 11 |
| | High RI | 14.2 ± 2.2 | 0.977 ± 0.054 | 7 |

**Table S2** The effects of $\gamma$-5 on the properties of homomeric and heteromeric AMPARs expressed in tsA201 cells (see Fig. 7a). Data from cells transfected with two AMPAR subunits were grouped according to the measured RI (see text for details).

| | Conductance (pS) ($n$, $P$) | $P_{o,\max}$ ($n$, $P$) | RI (+60mV/–80mV) ($n$, $P$) |
|---|---|---|---|
| GluR2(Q) | 19.4 ± 1.3 (10) | 0.40 ± 0.05 (9) | 0.052 ± 0.010 (10) |
| + γ-2 | 30.5 ± 3.7 (6, 0.0044) | 0.70 ± 0.02 (6, 0.001) | 0.120 ± 0.007 (6, 0.0004) |
| + γ-5 | 26.1 ± 1.8 (8, 0.0066) | 0.39 ± 0.05 (8, 0.8978) | 0.079 ± 0.018 (8, 0.1656) |
| GluR2L(Q) | 17.7 ± 1.8 (7) | 0.39 ± 0.01 (7) | 0.036 ± 0.008 (8) |
| + γ-2 | 26.4 ± 2.3 (6, 0.0129) | 0.69 ± 0.05 (6, 0.0275) | 0.201 ± 0.022 (4, <0.0001) |
| + γ-5 | 32.9 ± 3.3 (7, 0.0017) | 0.42 ± 0.09 (6, 0.8027) | 0.073 ± 0.016 (4, 0.0374) |

**Table S3** Comparison of effects of $\gamma$-2 and $\gamma$-5 on GluR2(Q) and GluR2L(Q) receptors (see Fig. 7b-d).